

Influence of magnetic field on two-phase flow convective boiling of some refrigerant mixtures

Samuel M. Sami^{*,†} and Joseph D. Comeau

Mechanical Engineering, Faculty of Engineering, University of Moncton, Moncton, NB, Canada E1A 3E9

SUMMARY

In this paper, an experimental study on the influence of magnetohydrodynamic (MHD) on heat transfer characteristics of two-phase flow boiling of some refrigerant mixtures in air/refrigerant horizontal enhanced surface tubing is presented.

Correlations were proposed to predict the impact of MHD on the heat transfer characteristics such as average heat transfer coefficients, and pressure drops of R-507, R-404A, R-410A, and R-407C in two-phase flow boiling inside enhanced surface tubing. In addition, it was found that the refrigerant mixture's pressure drop is a weak function of the mixture's composition.

It was also evident that the proposed correlations for predicting the heat transfer characteristics were applicable to the entire heat and mass flux, investigated in the present study. The deviation between the experimental and predicted value using new and improved correlations for the heat transfer coefficient and pressure drop were less than $\pm 20\%$, for the majority of data. Copyright © 2005 John Wiley & Sons, Ltd.

KEY WORDS: heat transfer; MHD; boiling; refrigerants mixtures

1. INTRODUCTION

The effect of magnetism and magnetic field on fluids is still considered as a not well known subject. However, it is well established that there are major changes caused by the passage of fluid through magnetic field.

Several studies reported in the literature demonstrated the magnetic field and its capabilities as well as its impact on the thermodynamic characteristics. However, as the electrical hydrodynamic (EHD) technique has shown an improvement of the heat transfer rate on refrigerant side (Sami and Aucoin, 2003), it is believed that magnetic field could have an enhancement effect on heat transfer properties.

The literature revealed that in addition to what has been reported by Sami *et al.* (1996, 1998, 2000, 2003), Wang *et al.* (1998) investigated nucleate boiling on several commercially available enhanced and smooth tubes using working fluids R-22, R-123, R-134a, R-407C and R-410A in

*Correspondence to: Samuel M. Sami, Mechanical Engineering, Faculty of Engineering, University of Moncton, Moncton, NB, Canada E1A 3E9.

†E-mail: samis@umoncton.ca

*Received 20 July 2004
Revised 11 December 2004
Accepted 26 January 2005*

water/refrigerant geometry. His work concluded that heat transfer coefficients of R-410A and R-22 are comparable. Other results have been reported on two-phase flow characteristics inside smooth tube by Wijaya and Spatz (1995) using R-22 and R-410A.

Numerous studies on the fluid flow and heat transfer of refrigerant mixtures inside horizontal smooth tubes by Sami and Aucoin (2003) and Khartabil *et al.* (1988), Heide and Schenk (1996), Krauss *et al.* (1996), Tanka and Sotani (1998), Webb *et al.* (1971) reported no remarkable effect of the mixture's composition on the flow pattern of condensation. However, none has been cited in the literature on influence of Magnetic Hydrodynamic (MHD) field on the heat transfer characteristics of refrigerant mixtures (Yata, 1998; Sami and Kita, 2005).

The present research work has been undertaken to better understand the impact of magnetic field on the boiling fluid flow and heat transfer characteristics of some new alternative refrigerant mixtures inside enhanced micro-fins surface tubing under various levels of magnetic flux: R-410A (R-32/R-125:50/50%), and R-407C (R-32/R-125/R-134a:23/25/52%). All percentages of the aforementioned blends are based on weight.

2. EXPERIMENTAL APPARATUS AND MEASUREMENTS

Figure 1 shows a schematic diagram of the experimental set-up, which is composed of an air/refrigerant vapour compression heat pump with 3 kW compressor.

Various magnetic elements with gauss level of 4000 each have been employed in this study. These magnets were clamped at the refrigerant lines, single-type with two brackets strapped

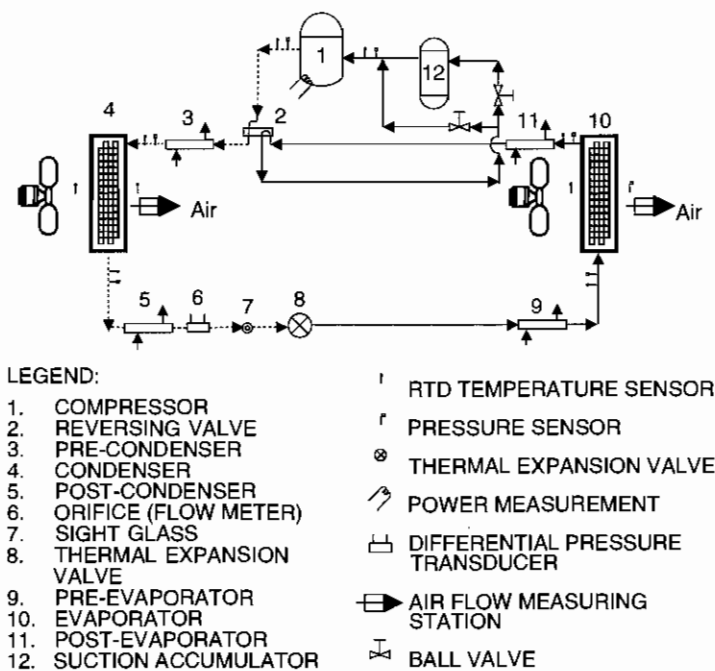


Figure 1. Schematic diagram of air/air heat pump test facility.

around the pipe. They were clamped on the refrigerant liquid line at the post condenser outlet at various distances, before the capillary tube/thermal expansion valve used as flow control device and at the low vapour pressure line leading to the compressor. The permanent magnets were placed at different locations of the outlet of post condenser. This was necessary to ensure that the magnets are placed on the refrigerant full liquid line. The full liquid line is defined as a section of the pipe where the flow is sub-cooled liquid. At each position, experiments were conducted with one, two and three or more magnets placed at 0.01 m spacing between each other. Figure 1 depicts the set up flow diagram and magnet positions.

2.1. Test facility

A test facility was constructed to study the refrigerant mixture boiling under liquid injection conditions. The facility was capable of producing saturated vapour at the evaporator outlet for boiling studies. The experimental set-up is an air/refrigerant vapour compression heat pump and is composed mainly of a 3 kW compressor, oil separator, condenser, pre-condenser, pre-evaporator, adjustable expansion device equipped with a series of capillary tubes with control valves, and a test evaporator. The oil content in the refrigerant loop was estimated to be about 1% using gas chromatography.

2.2. Test section

The experimental set-up test section was composed of a micro-fin finned evaporator coil. The geometry of the coils is presented in Tables I and II, whereas Table II gives details of the micro-fins geometrical parameters. Furthermore, Table III gives the test conditions and information on the key parameters of the system. Pressure, temperature and flow rate measuring stations are also shown in Figure 1.

The accuracy of the pressure transducers was $\pm 2.5\%$. Differential pressure transducers were employed to measure the refrigerant pressure drop. Temperatures were measured by RTD sensors with an accuracy of $\pm 0.5\%$ of full scale.

Table I. Air coils specification.

Tube outer diameter	0.375 in (0.9525 cm)
Rows deep	4
Fins per inch	12
Fins depth	3.6 in (8.884 cm)
Fins height	20 in (50 cm)
Fins length	30 in (76 cm)
Fins thickness	0.045 in (0.114 cm)
Rifled tubes	Micro-fins

Table II. Geometry of micro-fin tubes (round tip geometry).

Outside diameter	0.75 in (0.525 cm)
Root diameter	0.44 in (0.738 cm)
Tip diameter	0.31 in (0.407 cm)
Fins height	0.074 in (0.0188 cm)
Pitch	0.016 in (0.0406 cm)

Table III. Test conditions.

1	Temperature of air at the condenser inlet	21°C
2	Temperature of air at the evaporator inlet	-15°C to +8°C
3	Air flow rate	7.07×10^{-2} to $9.4 \times 10^{-2} \text{ m}^3 \text{ s}^{-1}$
4	Refrigerant mass flow rate	8–40 g s ⁻¹
5	Condenser pressure	600–1800 kPa
6	Evaporator pressure	170–450 kPa
7	Standard relative humidity at condenser inlet	45%

The accuracy of the mass flow measurements was $\pm 3\%$ of the nominal flow. Air temperatures data at inlet and outlet of the evaporator and condenser were stable experienced no fluctuations and therefore, a typical response time of RTD was sufficient and considered accurate for such an application.

In order to close the energy balance power supplied to the compressor and fans was measured with an accuracy of $\pm 2.5\%$.

2.2.1. Water loop. Water was circulated through the inside of the condenser tube to cool down the superheated refrigerant entering the condenser. The water loop was composed of pump, control valves, flow meter, and heat exchangers. The heat exchangers were used to provide accurate control of the water temperature before entering the condenser.

2.2.2. Anti-freeze loop. The anti-freeze solution was employed to remove heat from the refrigerant mixtures under investigation. The flow of anti-freeze was circulated through various components; subcooler, reservoir with immersed heater, water heat exchanger. The anti-freeze loop was capable of producing 3 ton of refrigeration at -18°C .

2.2.3. Data collection. Data collection was carried out using a P-130 equipped with a data acquisition system having a capacity of 112 channels. This enabled us to record with a single scan, local properties such as pressure drops, pressures, temperatures, flow rates, heat flux and power. All tests were performed under steady state conditions. The channels were scanned every second and stored every 10 s. The measured values were averaged over a period of 10 s.

In order to develop the proposed correlations describing the two-phase flow boiling heat transfer characteristics, the thermodynamic properties as well as transport properties of pure and zeotropic refrigerant mixtures should be known. The REFPROP version 6.01 Reid *et al.* (1987) and McLinden (1998) was used to evaluate the characteristics during phase change of the mixtures under investigation. On the other hand, interaction parameters were selected with caution to avoid influencing the transport properties of refrigerant mixtures (Sami and Poirier, 1998).

2.2.4. Test procedure. The results of the various refrigerant mixtures with no liquid injection were used as baseline for this study. Upon completion of the baseline results of each refrigerant mixture, under the aforementioned conditions, the compressor and the system were drained and evacuated. Following this step, the system was then recharged with the preferred refrigerant mixture. This procedure was repeated before conducting the series of tests for every single alternative mixture. Same type oil was used during experimentation.

During the experimentation, the sink air temperature was kept constant at 21°C, and relative humidity was also kept at 45%. The source coolant temperature varied from -15 to 5°C, at the evaporator inlet. The dry and wet bulb temperatures of the source and sink were within the ASHRAE and ARI Standards.

2.2.5. Saturated refrigerant conditions. The anti-freeze temperature at the test section was adjusted until the desired saturation conditions are achieved. The saturation temperature is controlled by the inlet anti-freeze temperature and flow as well as the immersed heater in the anti-freeze tank.

During the boiling testing the refrigerant mixture saturation temperature was compared with two temperatures refrigerant mixture probes in the test section. Saturation condition was considered achieved if the temperatures agree within $\pm 0.5\%$.

2.2.6. Uncertainty of the results. The convective boiling heat transfer coefficient is determined from the test section heat balance, temperature difference and other thermal resistances. Earlier experience with our instrumentation and current study showed that the uncertainty in the refrigerant side heat transfer coefficient was $\pm 7.5\%$ and overall heat transfer coefficient was $\pm 10.8\%$. For further details the reader is advised to consult references Sami and Poirier (1998) and Sami and Grell (2000).

3. MODELLING OF HEAT TRANSFER CHARACTERISTICS

In the following sections, the results of the heat transfer characteristics such as pressure drops, heat transfer coefficients at different conditions will be presented and discussed.

3.1. Heat transfer

The following equations have been employed to calculate the heat transfer coefficients from the data stored during each particular test at equilibrium conditions.

The heat transfer rate in the evaporator test section can be determined from the heat balance of the airflow;

$$Q_a = \dot{m}_a(H_{a\text{in}} - H_{a\text{out}}) \quad (1)$$

where $H_{a\text{out}}$ and $H_{a\text{in}}$ are the total enthalpies of airflow leaving and entering the evaporator, respectively.

The vapour quality at the exit of the test section was calculated from an energy balance of

$$x_{\text{out}} = x_{\text{in}} + \frac{Q_a}{\dot{m}_r h_{fg}} \quad (2)$$

the system and the refrigerant properties were determined at saturation conditions in the test section.

The total heat transferred to the refrigerant is

$$Q_{\text{rt}} = \dot{m}_r h_{fg} \Delta x \quad (3)$$

where Δx is the quality change in the test section.

The overall heat transfer coefficient based on the outside surface area of the test section is

$$U = \frac{Q_{rt}}{A_o \text{LMTD}} \quad (4)$$

where LMTD is the logarithmic mean temperature difference based on the inlet/outlet of air/refrigerant flows. The calculation of the LMTD is based on the nonlinear enthalpy variation with temperature. Furthermore, the LMTD was calculated for one straight section of the test section. No integration of LMTD values was needed, since only one section of the heat exchanger was considered in this study.

Assuming no fouling and R_{wal} is the thermal resistance in the copper wall of the tube, the refrigerant heat transfer coefficient h_r can be calculated as follows:

$$\frac{1}{h_r - A_i} = \frac{1}{UA_o} - \left(\frac{1}{h_a A_o} + R_{\text{wal}} \right) \quad (5)$$

where h_a is the air heat transfer coefficient and is calculated using the Wilson plot technique as described in Khartabil *et al.* (1988). R_{wal} is the wall resistance evaluated using the actual thickness and the outside diameter of the tube.

During the course of this study for data resolution purposes, the enhanced surface tube has been treated as a plain tube with an equivalent diameter. Using the equivalent diameter is consistent with the approach suggested by Sami and Poirier (1998) and Khartabil *et al.* (1988) for the enhanced surface tubing heat exchangers.

The reliability of the testing facility has been checked out by comparing the correlations reported by Collier (1981). Excellent agreement was obtained. Interested readers are advised to consult Sami and Desjardins (2000) for similar results on single phase, and two-phase flows of pure and/or refrigerant mixtures.

4. RESULTS AND DISCUSSION

4.1. Boiling characteristics

Samples of the experimental boiling data have been plotted in Figures 2–5, where the boiling heat transfer coefficient is plotted versus mass flow rate and the Reynolds number for various refrigerant mixtures. As expected, the data showed that the boiling heat transfer coefficient increases with the increase in the Reynolds number and the mass flow rate. The data clearly indicated that the boiling heat transfer coefficient was significantly influenced by the application of magnetic field. The heat transfer coefficient was enhanced using the magnetic field with some refrigerant mixtures as shown in Figures 2 and 3. However, some refrigerant mixtures did not respond to magnetic treatment equally. This is quite evident for certain flows and Reynolds number was less than 80 000. The impact of magnetic field on the heat transfer coefficient as well as the thermophysical properties was demonstrated via the various plots of Reynolds number and heat transfer coefficients.

It also appears from the data presented in Figures 2–5 that the magnetic field had a positive effect on the heat transfer coefficient of refrigerant mixtures with less gliding temperatures and moderate boiling temperatures such as R-404A and R-410A. In particular Figure 4 has shown that the magnetic field was insignificant at lower mass flow rates less than 0.02 kg l s^{-1} . On the

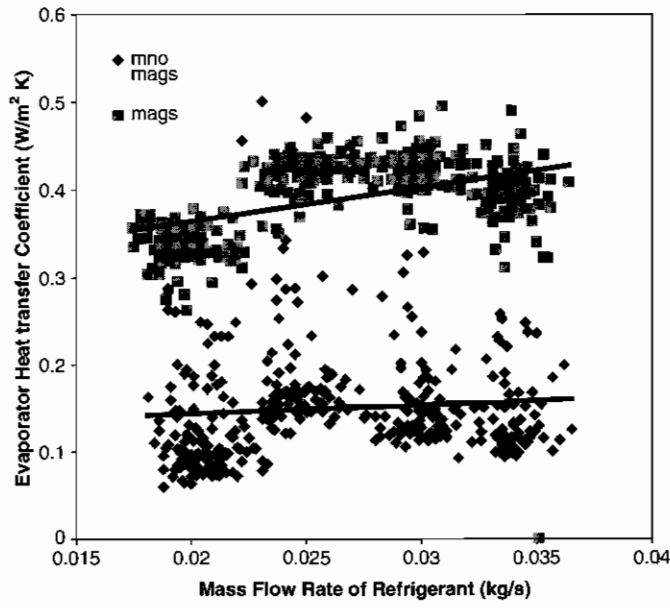


Figure 2. Display of boiling heat coefficient of R-404A versus mass flow rate.

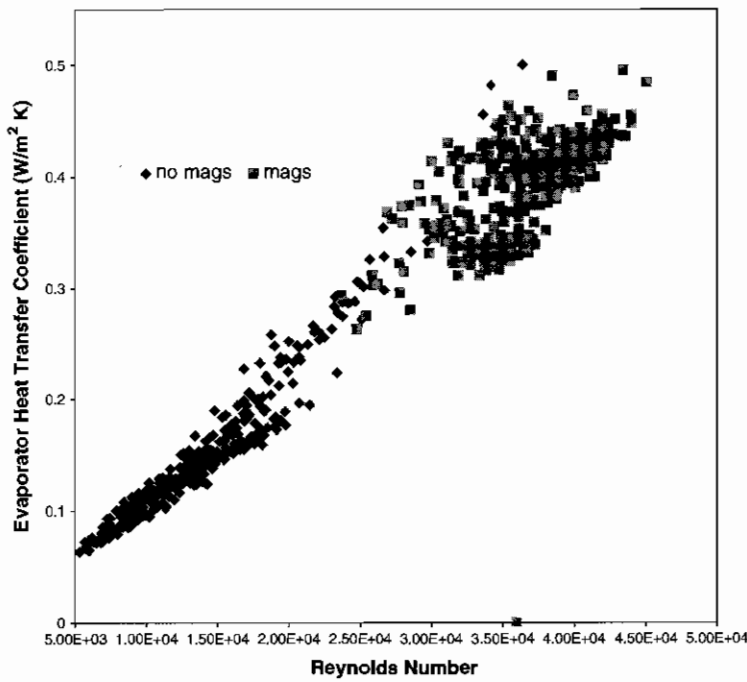


Figure 3. Heat transfer coefficient for R-404A at various Reynolds numbers.

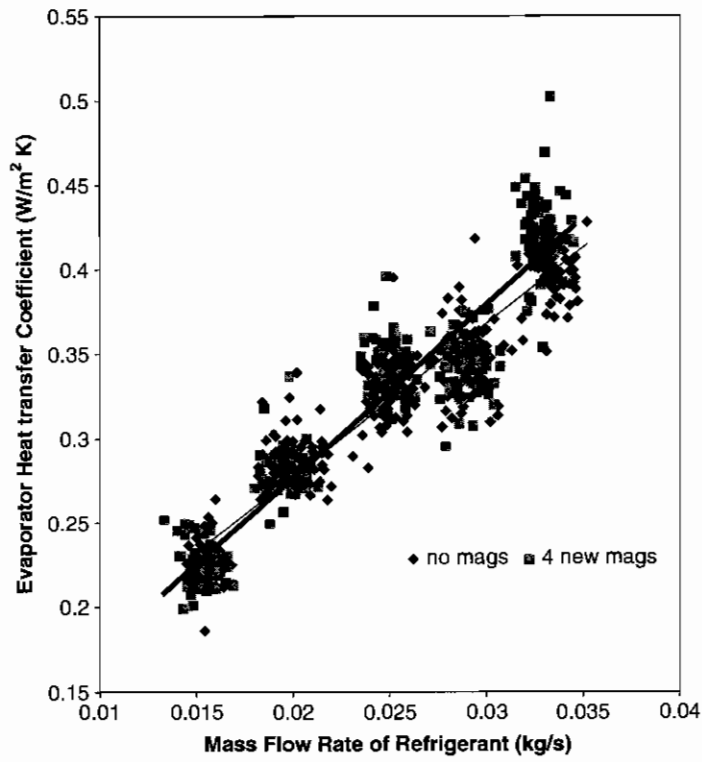


Figure 4. R-410A HTC versus mass flow rate.

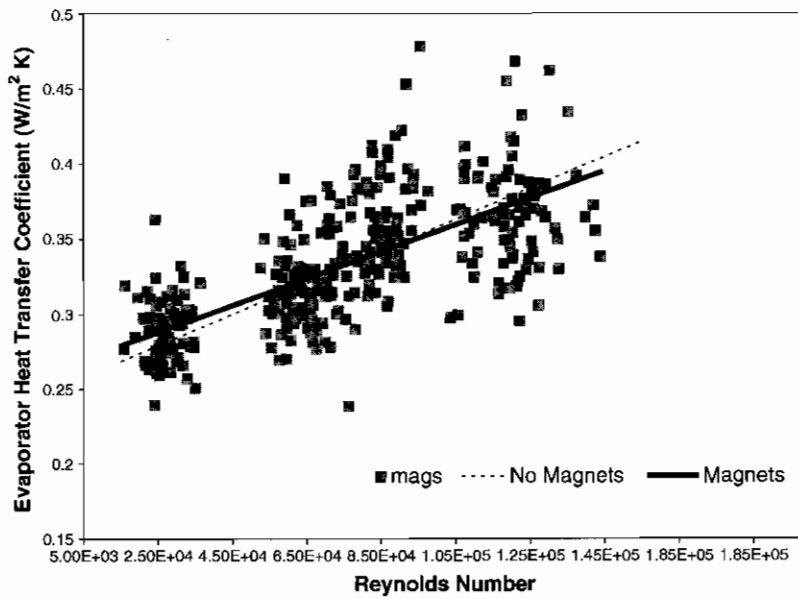


Figure 5. HTC of R-407C versus Reynolds number.

other hand, the results demonstrated that as flow rates increased the magnetic impact became evident.

The data displayed in the above-mentioned figures showed that the heat transfer coefficient was influenced by the Reynolds number, magnetic field power and the boiling point of the refrigerant mixture.

After detailed analysis of the convective boiling two-phase flow data, the following form proposed by Sami and Song (1996) is considered. Figure 7 showed the proposed correlation for R-410A:

$$Nu_e = A(Re^2 \cdot K_f)^{0.3} + B \tag{6}$$

where

$$Nu_e = \frac{hD_b}{k}, Re = \frac{GD_b}{\mu}, K_f = \frac{\Delta X h_{fg}}{L \cdot g}$$

And finally, Equation (6) takes the following form:

$$Nu_e = AY + B \tag{7}$$

Figure 7 had been constructed in an attempt to validate the proposed correlation, where values of measured heat transfer coefficients and nondimensional heat transfer coefficient predicted by the proposed correlation were compared with experimental ones for R-407C as a sample of the experimental data. The data plotted in these figures showed that the correlation is applicable to

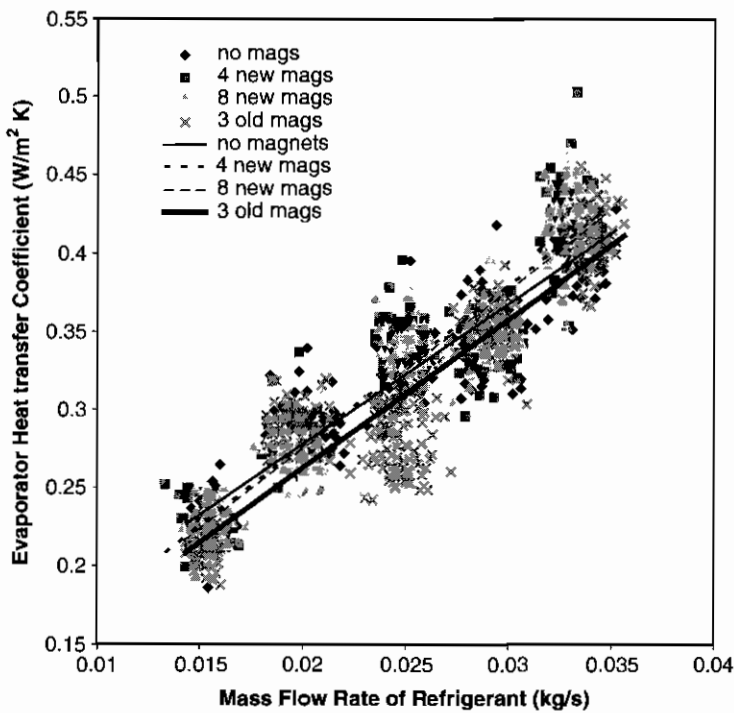


Figure 6. R-410A HTC versus mass flow rate.

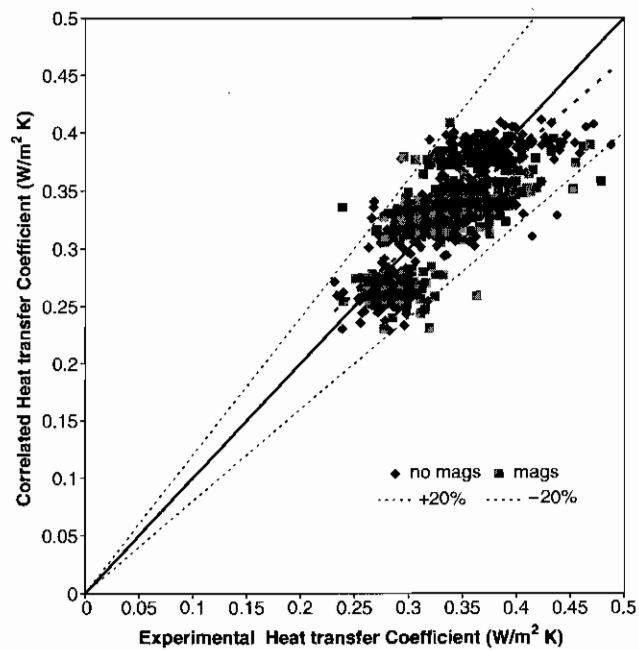


Figure 7. R-407C correlated versus experimental heat transfer coefficient.

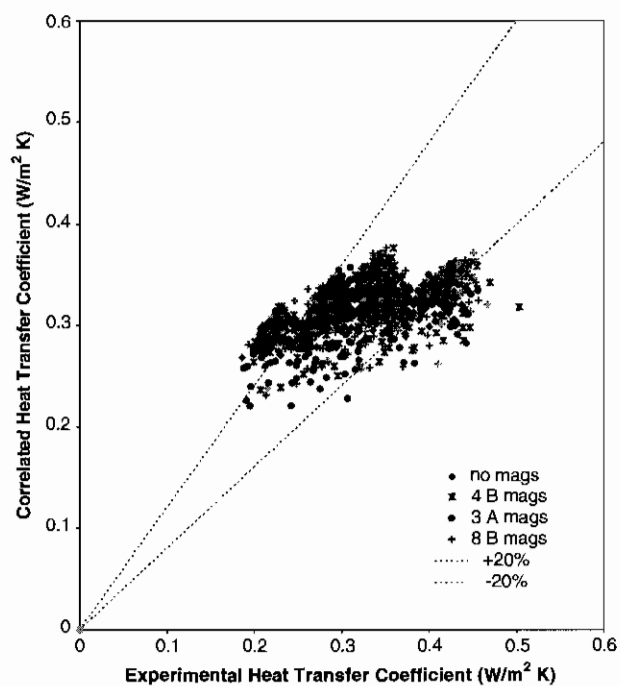


Figure 8. R-410A correlated versus experimental heat transfer coefficient.

the entire heat and mass flux, investigated in the present study for the proposed blends under question. The average deviation between the experimental and predicted values was less than $\pm 20\%$, for the majority of data. Similar deviations have been observed with the other refrigerant mixtures under investigation.

Another attempt has been made to validate the experimental data for R-410A and was presented in Figure 8. Other samples of R-507 are shown in Figure 9 where it appears that the average deviation between the experimental and predicted values was less than $\pm 20\%$, for the majority of data.

No attempts have been made to compare the proposed boiling correlations to existing ones, since to the authors' knowledge, none were reported in the literature under liquid injection test conditions.

Equation (7) clearly showed as presented in Figure 10 that there was a functional dependence of boiling heat transfer on the transport properties; and particularly thermal conductivity and viscosity of the refrigerant mixtures as well as other parameters. However, a sensitivity analysis demonstrated that the thermal conductivity and viscosity were the most crucial to the prediction of the boiling characteristics (Sami and Desjardins, 2000; Sami and Grell, 2000). Those thermophysical properties were significantly influenced by the MHD (Sami and Kita, 2004).

The proposed correlations in Equation (6) and their inherent dependence on the magnetic power have been plotted in Figures 6–10, where as the Nusselt numbers calculated after the experimental data obtained for the refrigerant mixtures in question was plotted against various numbers of magnets with different Gauss power. The comparison between the measured forced

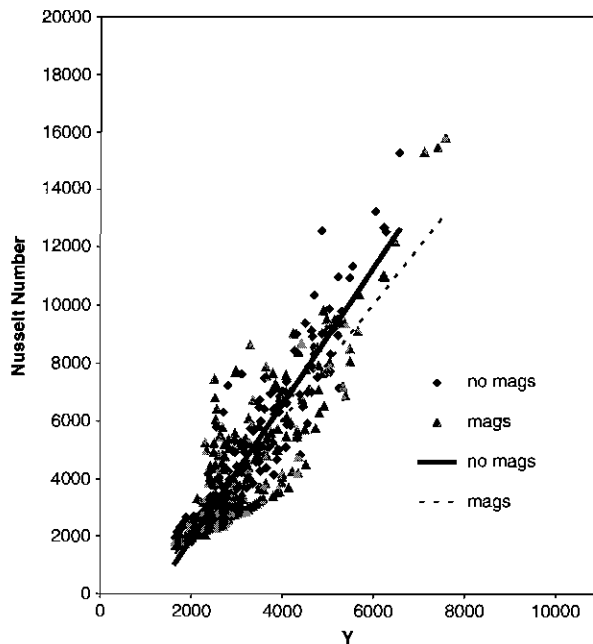


Figure 9. R-507 Boiling Nusselt number correlations.

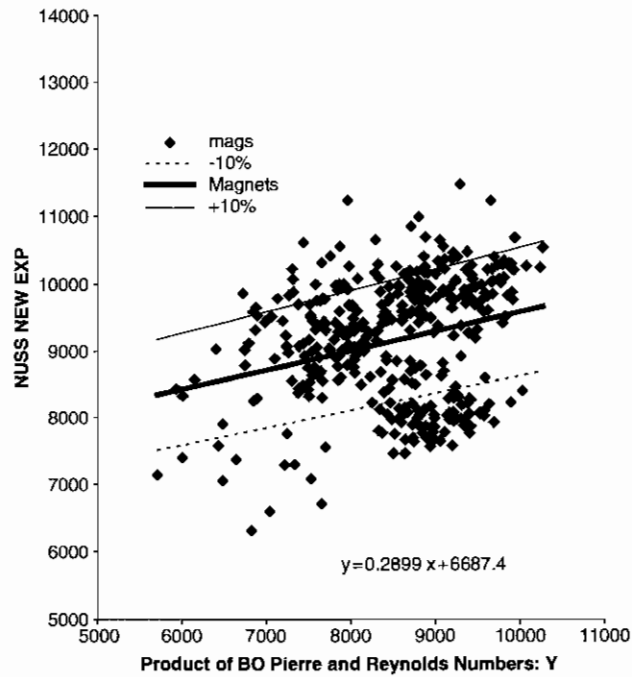


Figure 10. Validation of the data for R-401A.

convection boiling heat transfer coefficients showed that the data displayed was applicable to the entire heat and mass flux range for the proposed blends under question.

5. CONCLUSIONS

The boiling heat transfer coefficient characteristics of some alternatives refrigerant mixtures such as R-404A, R-407C, R-507, and R-410A have been studied in air/refrigerant under magnetic field conditions. The data revealed that magnetic treatment is beneficial to the heat transfer coefficient depending upon the Reynolds number and the boiling point as well as the type of refrigerant.

In addition, the proposed heat transfer coefficient correlations were found to be applicable to the entire heat and mass flux, in the present study under the gas/liquid injection conditions. The deviation between the experimental and predicted under liquid injection was less than $\pm 20\%$ for the majority of data.

NOMENCLATURE

A = heat transfer area (m^2)
 D = diameter of tube (m)

D_e	= equivalent diameter based on the bore diameter ($D_e = D_{oi} - D_{bo}$) (m)
D_{bo}	= fin height (m)
D_{oi}	= outside diameter (m)
G	= mass flux ($\text{kg m}^{-2} \text{s}^{-1}$)
h	= heat transfer coefficient ($\text{kW m}^{-2} \text{K}^{-1}$)
h_{fg}	= latent heat of vaporization (kJ kg^{-1})
H	= total air enthalpy (kJ kg^{-1})
K	= thermal conductivity of liquid ($\text{kW m}^{-1} \text{K}^{-1}$)
L	= length (m)
\dot{m}	= mass flow rate (kg s^{-1})
P	= pressure (kPa)
Q	= heat input (kW)
R_{wal}	= wall thermal resistance (K kW^{-1})
T	= temperature ($^{\circ}\text{C}$ or K)
U	= overall heat transfer coefficient ($\text{kW m}^{-2} \text{K}^{-1}$)
x	= quality based on mass (dimensionless)
Z	= characteristic length (m)

Greek letters

μ	= viscosity of liquid (Pa s)
ρ	= density (kg m^{-3})

Dimensionless numbers

K_f	= Bo Pierre boiling number ($\Delta x h_{fg}/gL$)
Nu	= Nusselt number (hD_e/K)
Nu_e	= Nusselt number for evaporation (hD_b/K)
Re	= Reynolds number (GD_e/μ)
Re_L	= Reynolds number for boiling ($\rho_l u_{\text{vin}} L/\mu$)

Subscripts

a	= air
ac	= acceleration
av	= average
b	= bore
e	= equivalent
en	= entrance
ex	= experimental
i	= inside
in	= inlet
L	= liquid
m	= measured
o	= outside
out	= outlet

r	= refrigerant
rt	= transferred to refrigerant
tp	= two-phase
v	= vapour
wal	= wall

ACKNOWLEDGEMENTS

The research work presented in this paper was possible through grants from NSERC. The authors wish to acknowledge the continuous support of the University of Moncton.

REFERENCES

- Collier JG. 1981. *Convective Boiling and Condensation* (2nd edn). McGraw-Hill Book Co.: New York.
- Heide R, Schenk J. 1996. Bestimmung der Transportgrossen von HFKW, Heft 1, Viskosität und Oberflächenspannung. *Bericht zum AiF-Forschungsvorhaben Nr. 10044B*, Forschungsrat Kältetechnik e.V., Frankfurt, März.
- Khartabil HF, Christensen RW, Richards DE. 1988. A modified Wilson plot technique for determining heat transfer correlations. *2nd U.K. National Conference on Heat Transfer*, University of Strathclyde, Glasgow, England, 14–16 September.
- Krauss R, Weiss VC, Edison TA, Stephan K. 1996. Transport properties of 1,1-difluoroethane (R-152a). *International Journal of Thermophysics* **17**(04):731–757.
- McLinden MO. 1998. *NIST Thermodynamic and Transport Properties of Refrigerant Mixtures*, Version 6.01. NBS: Gaithersburg, MD.
- Reid RC, Prausnitz JM, Poling BE. 1987. *The Properties of Gases and Liquids* (4th edn). McGraw-Hill: New York.
- Sami SM, Aucoin S. 2003. Effect of magnetic field on the performance of new refrigerant mixtures. *International Journal of Energy Research* **27**(3):203.
- Sami SM, Desjardins D. 2000. Boiling characteristics of ternary mixture inside enhanced surface tubing. *International Communications in Heat and Mass Transfer Journal* **24**:1359.
- Sami SM, Grell J. 2000. Heat transfer prediction of two phase flow boiling of alternatives to R-22. *International Journal of Energy Research* **24**:349.
- Sami SM, Kita R. 2005. Behaviour of new refrigerant mixtures under magnetic field. *International Journal of Energy Research*, 2005, in press.
- Sami SM, Poirier P. 1998. Prediction of forced convective condensation characteristics of new alternatives to R-502 inside water/refrigerant enhanced surface tubing. *ASHRAE Transactions* **105**(Pt. 1).
- Sami SM, Song B. 1996. Heat transfer and pressure drop characteristics of HFC quaternary refrigerant mixtures inside enhanced surface tubing. *Applied Thermal Engineering* **16**(6):461.
- Tanka Y, Sotani T. 1998. Survey of viscosity data for HFC refrigerants and their mixtures. *Manuscripts for IEA Annex-18*, Meeting held on June 8, 1998 at SINTEF, Trondheim, Norway.
- Wang C, Shieh W, Chang Y. 1998. Nucleate boiling performance of R-22, R-123, R-134a, R-410A, and R407C on smooth and enhanced tubes. *ASHRAE Transactions* **104**(Pt. 1).
- Webb RL, Eckert ERG, Goldstein RJ. 1971. Heat transfer and friction in tubes with repeated-ribs. *International Journal of Heat and Mass Transfer* **14**:601.
- Wijaya H, Spatz M. 1995. Two-phase flow heat transfer and pressure drop characteristics of R-22 and R32/R125. *ASHRAE Transactions* **101**(Pt. 1).
- Yata J. 1998. A survey of the thermal conductivity of HFC mixtures. *Report prepared for the IEA Annex-18*, Meeting held on June 8, 1998 at SINTEF, Trondheim, Norway.
- Zurcher O, Thome JR, Favrat D. 1998. In-tube flow boiling of R-407C and R-407C/oil mixtures. Part I: microfin tubes. *HVAC&R Research* **4**(4).